Design of a Dynamic Grain Flow Model for a Combine Harvester

Maertens, K.; Reyniers, M.; De Baerdemaeker, J.

Laboratory for Agro-Machinery and Economics
Kasteelpark Arenberg 30, B-3001 Leuven (Belgium)
Phone: ++32-16321444 Fax:++32-16321994
Email: Koen.Maertens@agr.kuleuven.ac.be

ABSTRACT

Nowadays, commercial grain flow sensors are available for each type of combine harvester. Based on this signal and other site-specific data, grain yield maps are produced, revealing local field characteristics. In contrast to the technology of these sensors, the data processing part is not optimized yet. Former studies show how significantly the combine harvester smooths feedrate variations and by this, bounds the accuracy of constructed grain yield maps.

An analytical grain flow model is constructed based on physical insight and experimental data of selected machine sections. From this non-linear high order model, a low order linear model for the frequency band of interest is extracted. An optimal linear model which has algebraic compensation for the internal return loop, estimates the grain feedrate of the harvester.

Once the dynamic behavior of the harvester is known in a simple, linear form, model-based grain yield estimations can be constructed, that may be used to improve the quality of constructed grain yield maps.

Keywords: Machine dynamics, Combine harvester, Model-based signal processing, Yield mapping

1. INTRODUCTION

Online grain flow measurement is particularly interesting because of its direct relationship with site-specific yield. While clean grain flow is only measured at the end of the threshing and cleaning process, that is also the ideal position for flow measurement. Nevertheless, that location has an important drawback. The estimation of the feedrate by means of an output measurement is irreversibly affected by the dynamics of the machine itself. Studies on the impact of this effect (Blackmore & Moore, 1999) and feasible solutions (Birrell *et al.*, 1996; Vansichen & De Baerdemaeker, 1992; Searcy *et al.*, 1989) have been formulated without much success. The latter correction methods are generally based upon the inverse application of a first or second order filter. These black box models are identified by introducing limiting assumptions about the so far not-measurable input grain flow and local yield on the field together with the choice for dynamic parts of the output flow such as the beginning and end of a harvest run or artificial machine speed variations.

Maertens, K., M. Reyniers, and J. De Baerdemaeker. “Design of a Dynamic Grain Flow Model for a Combine Harvester”. Agricultural Engineering International: the CIGR Journal of Scientific Research and Development”. Manuscript PM 01 005. Vol. III.

These suppositions and special signals explain the difficulties of inverse filtering since they do not represent all harvest conditions.

The other possible approach to construct a grain flow model is the analytical way. Basic components of the machine such as the collector augers and elevators can be modeled by simple integrators and time delays. Other more complex sections as the threshing (Gregory & Fedler, 1987; Trollope, 1982) and cleaning units (Huynh & Powell, 1978) have already been studied.. Connecting these individual models produces a non-linear, high order description of the total machine influence (Maertens et al., 2001a; Fig.1).

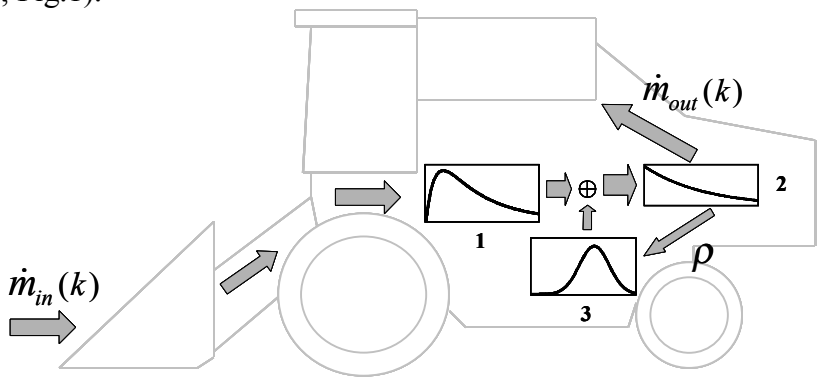

Figure 1. Schematic overview of the grain flow through combine harvester along with the main distributions on the grain path: 1) Spreading of the separated grain kernels along the grain pan, 2) cleaning of kernels from chaff and short straw ends and 3) spreading or return flow by impellers on the ends of the return auger

The way grain kernels are processed is dependent on the type of harvester. The study was performed on a New Holland *TX64®* combine harvester. Simular conclusions can be assumed for other types of harvesters. The most important parameters influence the combine harvester dynamics are the speed V_g of the grain kernels moving across the grain pan (1) and the fraction return flow ρ separated at the end of the sieving section (2) and which is spread across the grain pan by impellers (3) installed at the end of the return augers on the left side of the machine.

2. NON-LINEARITIES OF MACHINE DYNAMICS

Two major non-linear distortions are present in the machine influence on the incoming grain flow variations. Both cleaning and threshing units display significantly different throughput curves for changing feedrates. Figure 2 illustrates this effect for the threshing drum as a function of the separation length. Analogous curves can be found for other crop varieties, crop conditions and machine configurations. The left part shows the fraction separated grain kernels along the concave of the drum. These curves are obtained from an experimental set-up where separated grain kernels are collected in five different sections along the concave. A differentiable parametric model (Trollope, 1982) connects the measured cumulative separation fractions (**x**) and makes it possible to calculate the related probability function (pdf). The latter function is plotted for different feedrates and reveals clearly its influence. From a certain feedrate level, the first part of the concave starts to

saturate and extra offered material is processed further away from the start of the concave. As a result, the separation is more spread to the end of the separation area, resulting in a flattened shape of the pdf.

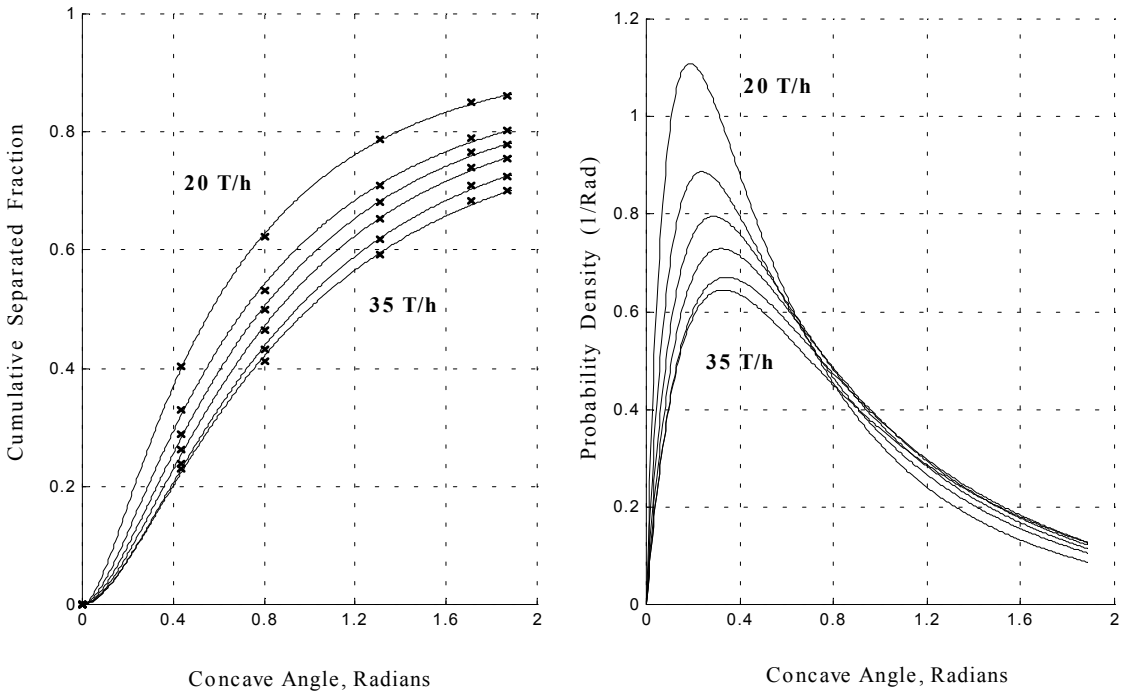

Figure 2. Cumulative separation and probability density function for the separation of grain kernels in function of concave angle (Radians) for different feedrates (20, 25, 28, 30, 32, 35 T/h)

The way this non-linear characteristic is translated into a global, dynamic non-linear behavior is illustrated in figure 3. The pdf of the individual drums are projected

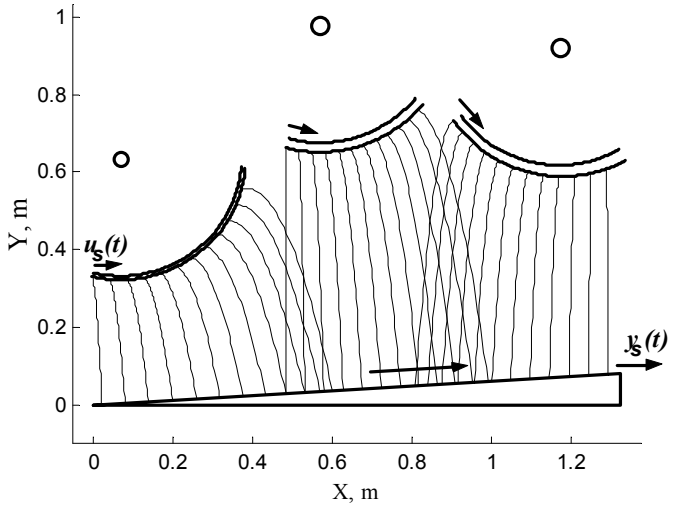

Figure 3. Trajectories of grain kernels separated in the three-series separation drums. Variables $u_s(t)$ and $y_s(t)$ are denoting respectively the input and output grain flow of the threshing section

on the grain pan through the grain kernel trajectories, putting together on e global separation pdf $P_g(x,u_s(t))$ for separated grain kernels as a function of distance x(m) from the front end of the grain pan and feedrate $u_s(t)$ (T/h) of the subsystem. Since the material speed through the threshing drum is much higher in comparison to the transport speed V_g (m/s) across the grain pan, the separated grain flow $y_s(t)$ (T/h) leaving the threshing section can be modelled by.

$$y_s(t) = \int_0^{L_g} P_g\left(x, u_s(t - \frac{L_g - x}{V_g} - \Delta T_{traj})\right) u_s(t - \frac{L_g - x}{V_g} - \Delta T_{traj}) dx \quad (1)$$

Where ΔT_{traj} is the mean transport delay (s) for a grain kernel moving from the entry of the threshing drum to the grain pan and L_g denotes the length (m) of the grain pan.

The global separation function $P_g(x,u_s(t))$ depends on different parameters besides feedrate $u_s(t)$. The most significant influences are grain/straw ratio, straw length, straw moisture, straw strength and variety. In case of normal crop conditions, this distribution function can be predicted based on measurable feedrates of the harvester (Maertens and De Baerdemaeker, 2001).

The same kind of non-linearity can be found for the cleaning unit. When higher feedrates are offered at this machine section, the throughput pdf is also shifted backwards, resulting in a non-linear cleaning process.

3. FREQUENCY ANALYSIS AND IDENTIFICATION

In the previous paragraph, an illustration was given to show how experimental results translated into relatively simple mathematical forms as in equation 1. For one section, the dynamic impact on the grain flow can be physically interpreted. When the different sections are put together, the influence in frequency domain is unpredictable and difficult to write into a low order mathematical formula ready to use for signal processing. *Simulink®* is need to build a global model and simulations are carried out with specific feedrate variations, exciting the total dynamics of the system.

To analyse a linear system in its frequency domain, an excitation signal is applied on the model, an output signal recorded and a frequency response function (FRF) is set up via Discrete Fourier Transforms $\dot{M}_{in}(k)$, $\dot{M}_{out}(k)$ of respectively input feedrate $\dot{m}_{in}(k)$ and output flow $\dot{m}_{out}(k)$:

$$FRF(k) = \frac{\dot{M}_{out}(k)}{\dot{M}_{in}(k)} = \hat{G}_O(j\omega_k) = G_O(j\omega_k) + N_G(j\omega_k) \quad (2)$$

For linear systems this function is independent on the excitation signal and by this, *FRF* gives a good non-parametric approximation $\hat{G}_O(j\omega_k)$ of the linear system $G_O(j\omega_k)$ for discrete frequencies ω_k. $N_G(j\omega_k)$ in eq.2 corresponds with the frequency representation of the stochastic error on the *FRF*-estimation.

This method of reasoning will not work if there are non-linear distortions present in the system. Other input feedrates will deliver other *FRF*-estimations, questioning the physical interpretation of the frequency function. In case of non-linear systems, *FRF* can be decomposed as (Schoukens *et al.*, 1998):

$$FRF = G_R(j\omega_k) + G_S(j\omega_k) + N_G(j\omega_k) \quad (3)$$

With

$$G_R(j\omega_k) = G_0(j\omega_k) + G_B(j\omega_k) \quad (4)$$

Where $G_R(j\omega_k)$ denotes the best linear approximation of the system consisting of the true underlying linear system $G_O(j\omega_k)$ and a bias term $G_B(j\omega_k)$ of the non-linear distortion. $G_S(j\omega_k)$ of eq.3 represents the stochastic non-linear part of the model. To find the best linear approximation, an averaging process should be introduced removing the stochastic components $G_S(j\omega_k) + N_G(j\omega_k)$ from the frequency response function. This can be obtained by applying different realizations of the same input spectrum $\dot{M}_{in}(k)$. An averaged output spectrum $\dot{M}_{out,R}(k)$ of the different simulations provides the best linear approximation.

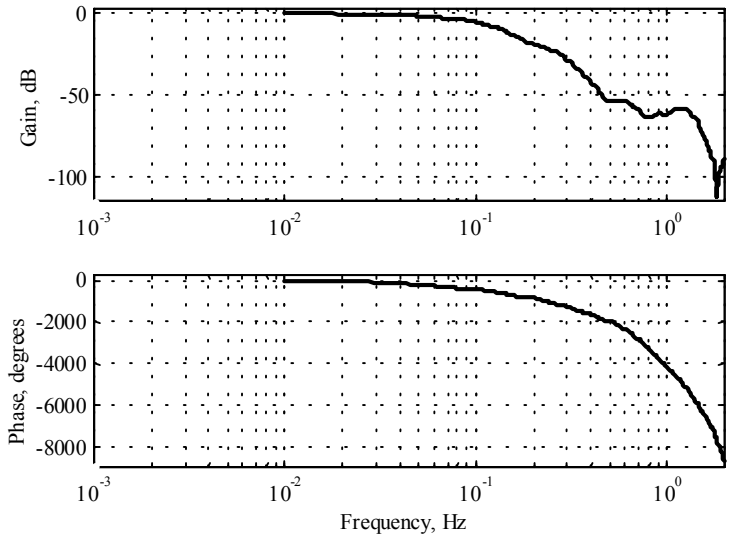

Figure 4. Best linear approximation $G_R(j\omega_k)$, for an excitation band of 0.01 to 2Hz and 0% return flow (Maertens et al., 2001b)

Figure 4 shows the result, realized with different multisines ($\dot{M}_{in}(k)$ =constant) for a frequency band of 0.01 to 2 Hz and a 0% return flow fraction. The average feedrate is chosen accordingly to a nominal feedrate of the machine. The resulting low pass characteristic is obvious and a value for the 3 dB point (=attenuation ratio of 0.5) at 0.075 Hz illustrates the significance of the dynamic impact. When the combine harvester travels at a speed of 1 ms^{-1}, spatial variations with wavelengths of 13.3 meters are already divided into halves. The high values of the phase characteristic are due to the relatively long minimal transport delay ΔT_{delay} of the grain transport from the entry up to the end of the process where the flow is measured.

To use this linear approximation in signal processing, a parametric model must be extracted. Since grain flow measurements are typically measured at a sample rate of 1Hz and are distorted by high frequency noise, it is only useful to identify an accurate model for low frequencies. The result of a frequency domain identification, carried

out with a least squared estimator and fixed constraints on the steady state gain (TF(0)≡1) and dead time ($\Delta T_{delay} \equiv 9$ s) is given by:

$$TF(s) = \exp(-9s)\frac{-0.06s+1}{3.1s^4+7s^3+7.6s^2+4.3s+1} \tag{5}$$

The fixed steady state constraint is applied because of physical reasons: a constant input flow should deliver the same constant output. An integer value for the time delay is enforced because of an easier conversion to discrete time. Making use of Tustin's conversion rule: s→ $2(1-q^{-1})/[T_s.(1+q^{-1})]$, the discrete time version of the model for a 1 Hz sample rate (T_s=1s) gives

$$G(q^{-1}) = q^{-9}\frac{0.0376q^{-1}+0.0304q^{-2}+0.002q^{-3}}{1-2q^{-1}+1.6q^{-2}-0.63q^{-3}+0.1q^{-4}} \tag{6}$$

with

$$\dot{m}_{out}(k) = G(q^{-1})\dot{m}_{in}(k) \tag{7}$$

describing the relation between the measured output flow $\dot{m}_{out}(k)$ (T/h) at the end of the process and the input mass flow $\dot{m}_{in}(k)$ (T/h) at the entry of the machine for a 0% return flow.

4. SIMPLIFIED RETURN LOOP SYSTEM

The transfer function $G(q^{-1})$ describes the filtering impact of the machine on feedrate variations of $\dot{m}_{in}(k)$ for the particular case of no return flow. Measurements with other return flows can be reduced to this special case after implementing the inverse version of the simplified return loop (Fig.5).

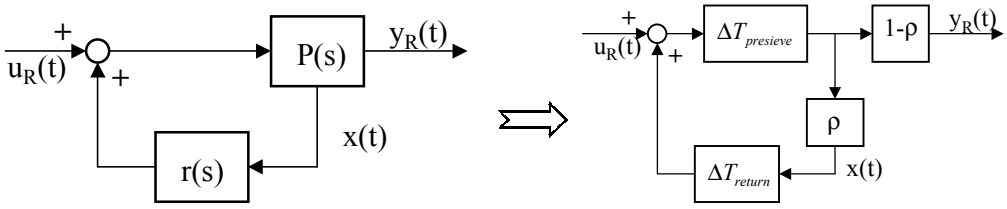

Figure 5. Generalised return loop system with separation transfer matrix *P(s)* and return flow dynamics *r(s)* together with its simplified version consisting of 2 time delays and 1 separator (Maertens et al., 2001b)

The influence of the return loop, consisting of a dynamic separation section, modeled by the matrix transfer function *P(s)* and the dynamics of the return loop *r(s)* can be approximated by 2 time delays $\Delta T_{presieve}$ and ΔT_{return}, and a separator, dividing the forward flow in a return fraction ρ and a clean fraction, *1-*ρ. For this simplified version, $u_R(t)$can be written in function of $y_R(t)$ by:

$$u_R(t-\Delta T_{presieve}) = \frac{1}{1-\rho}y_R(t) - \frac{\rho}{1-\rho}y_R(t-\Delta T_{presieve}-\Delta T_{return}) \tag{8}$$

Equation 8 gives the possibility to reduce all output flow measurements to the special case of 0% return flow, extending the application domain of $G(q^{-1})$. Analogously, output flow $y_R(t)$ can be written in function of input flow $u_R(t)$.

5. MODEL BASED GRAIN YIELD ESTIMATION

The frequency response function of fig.4 has proven the significant dynamic influence of the combine harvester on the incoming feedrate variations. Therefore, actual grain yield variations will be smoothed before the grain flow measurement is carried out. This effect reduces the value of the resulting grain yield map drastically. Generally, two methods can be used to estimate the local grain yield: application of inverse dynamics and filtering of surface flow.

To estimate the instantaneous grain yield *y(k)*, at least three parameters must be measured when process model $G(q^{-1})$ is available:

- Actual cutting width *w(k)*
- Ground speed *v(k)*
- Output grain flow $\dot{m}_{out}(k)$

The unmeasurable input grain flow $\dot{m}_{in}(k)$ can be formulated in function of above parameters by

$$\dot{m}_{in}(k) = y(k)w(k)v(k) = y(k)s(k) \tag{8}$$

Where *s(k)* denotes the surface harvested each second. Taking into account the dynamic relationship between input and output flow (Eqn.7), the dynamic relation between the measurable parameters and grain yield *y(k)* is given by

$$\dot{m}_{out}(k) = G(q^{-1})\mathbf{Z}\left(y(k)s(k)\right) \tag{9}$$

The $\mathbf{Z}$ -transform is written explicitly to accentuate the order of transformation.

5.1. Application of inverse dynamics $G^{-1}(q^{-1})$

The straightforward method to implement dynamic compensation is to make use of the compensation for the return flow influence (eq.8) and the inverse of the machine dynamics for a 0%-return flow fraction. The structure of this compensation is shown in figure 6. Since the machine dynamics exhibit a low pass behavior, the application of the inverse dynamics will result in an amplification of the high frequency noise on

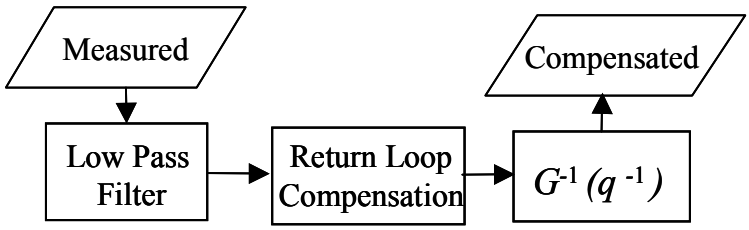

Figure 6. Inverse dynamics as compensation for machine dynamics

the grain flow measurement. Therefore, a low pass Butterworth filter must be installed to remove this noise without distortion of the low frequency content. Measurements on a New Holland TX64 combine harvester have shown that the cut off frequency of the low pass filter lies around 0.125 Hz. The actual grain yield compensation $\hat{y}_1(k)$ is realized by relating the compensated grain flow with the measured surface flow *s(k)*.

The essential part of this method is the invertibility of $G(q^{-1})$. When this is not the case, this method cannot be applied. The expansion of this method towards more complex, non-linear models or the implementation of other influence parameters is not straightforward.

5.2. Filtering of surface-flow

Short time grain flow variations are mostly caused by machine accelerations or cutting width alterations. Feedrate changes due to the natural spatial variability (Van Meirvenne et al., 1990) are smoother because of the limited machine speed in normal working conditions (< 2m/s). Under the assumption abrupt grain flow variations are supposed to come from *s(k)*-variations, the following new estimation can be set up for *y(k)* (Maertens et al.,2000):

$$\hat{y}_2(k) = \frac{\dot{m}_{out}(k)}{\mathbf{z}^{-1}\left\{G(q^{-1})s(k)\right\}} \tag{10}$$

In contrast with the method of the inverse dynamics, no extra low pass filter should be installed, since the $\hat{y}_2(k)$-estimation is robust towards high frequency noise on the measured signals. The remaining noise on the estimation will be removed in a final step when geostatistical interpolation techniques will be used to construct grain yield maps from point data. For this type of dynamic compensation, no inverse model must be calculated. Each type of model, linear or non-linear can be used for this grain yield estimation.

6. RESULTS AND DISCUSSION

Evaluation of the constructed grain flow model and corresponding grain yield estimation is difficult since no accurate grain feedrate measurements are available. To evaluate the grain yield estimation, a site-specific fertilized field is designed. Within each rectangular plot, the crop condition is kept as constant as possible. Before the time of harvest, one metre of crop was removed between each plot. By this, an abruptly varying feedrate is encountered during harvest.

6.1. Time domain analysis

The result of the first dynamic compensation is shown in figure 7. First, a low pass filter with a cut off frequency of 0.125 Hz is applied on the measured sequence, removing the high frequency signal content. Afterwards the inverse dynamics are

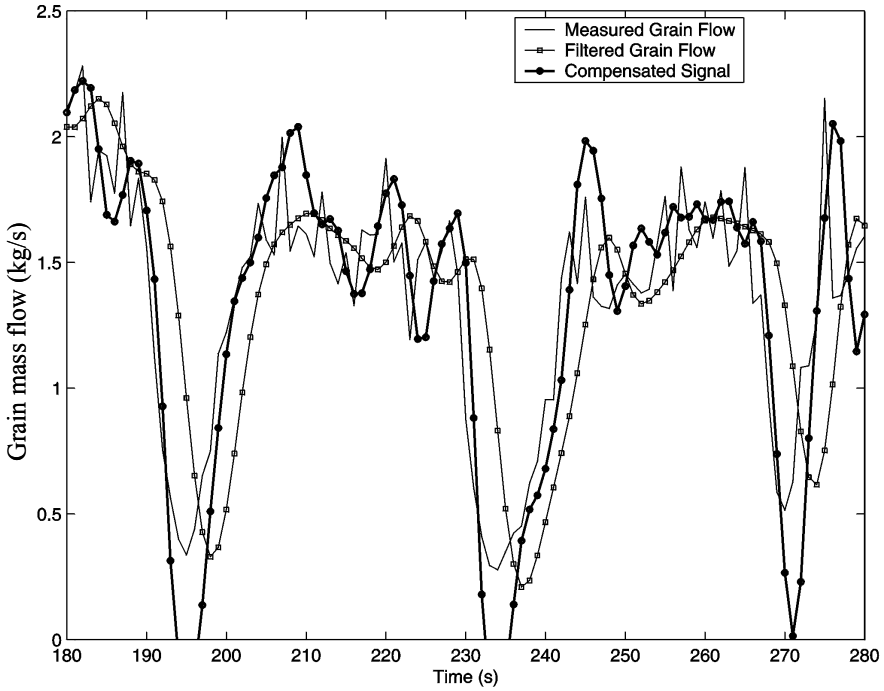

Figure 7. Time domain representation of different steps in $\hat{y}_1(k)$ grain yield estimation: Measured grain flow, filtered with low pass Butterworth filter and the final compensation after application of the inverse dynamics

applied, removing partially the smearing influence of the machine on the grain flow measurement. Although, an improvement is visible, still the step responses are not pulled straight fully. A perfect solution is not possible since the high frequency content is too much perturbed by measurement noise. With this method, feedrate variations from all kinds of sources (speed, cutting width or natural yield variations) will be corrected naturally. Since the partially compensated flow is referred to sharp surface variations, detecting whether the harvester is in or out the crop is critical.

Figure 8 illustrates the components of the $\hat{y}_2(k)$ grain yield estimation. The original surface flow *s(k)* is shown together with the output mass flow $\dot{m}_{out}(k)$ shifted across a constant time delay. The abrupt downward peaks of *s(k)*, indicating where the machine passes over the preharvested strips of crops, are filtered out by the grain flow model in the same way the combine harvester has filtered out the feedrate variations. In the first part of the signal (timestep 584), the measured grain flow increases rapidly, due to a

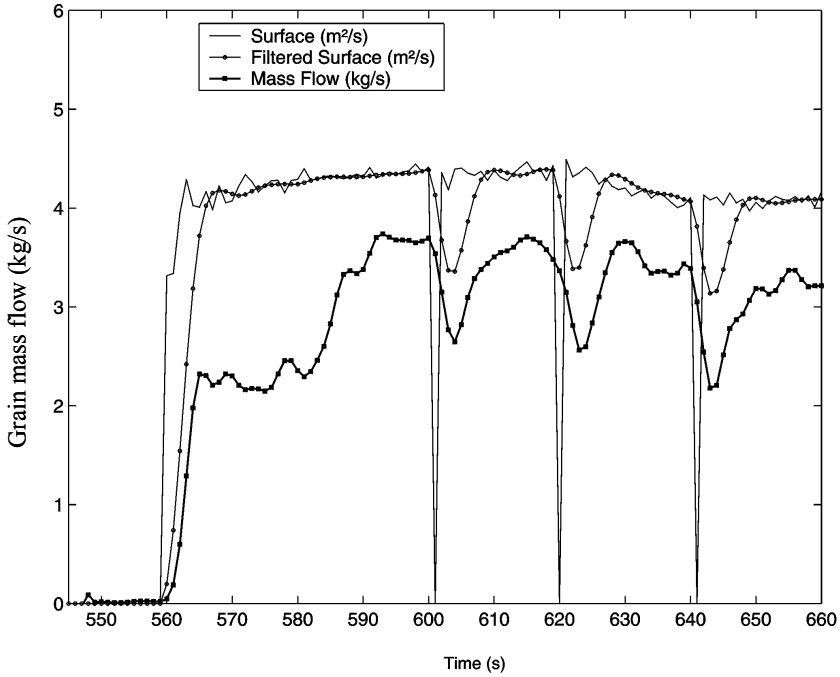

Figure 8. Signals constructing the $\hat{y}_2(k)$ yield estimation: Measured surface flow $s(k)$, filtered surface flow $Z^{-1}\{G(q^{-1})s(k)\}$ and measured output grain flow $\dot{m}_{out}(k)$.

natural variation of the grain yield. This method does not deliver any dynamic compensation for this feedrate step in contrast with the first grain yield estimation. Both flow signal and reference signal are smoothed. This makes the in/out detection less critical in comparison with previous grain yield estimation.

6.2. Spatial analysis

As a final result, grain yield maps are calculated with the classical method of shifting back the grain flow signal across an optimal time period and the model based approach by filtering the surface flow to compose the $\hat{y}_2(k)$ yield estimation. Figure 9 shows both maps next to each other. On the upper yield map, constructed with an appropriate timeshift, the driving directions of the combine harvester are marked. A good agreement is visible with the color variation within each plot. When the harvester enters each plot, the flow has not raised towards its steady state level, resulting in low yield estimations. At the end of a plot, the local yield is overestimated since the measured surface flow decreases faster than the grain flow. The lower figure illustrates the impact of the model based grain yield estimation on the resulting yield map. The transition zones are reduced, within each plot, the variation of the grain yield is much lower, although the grain flow signal is not smoothed.

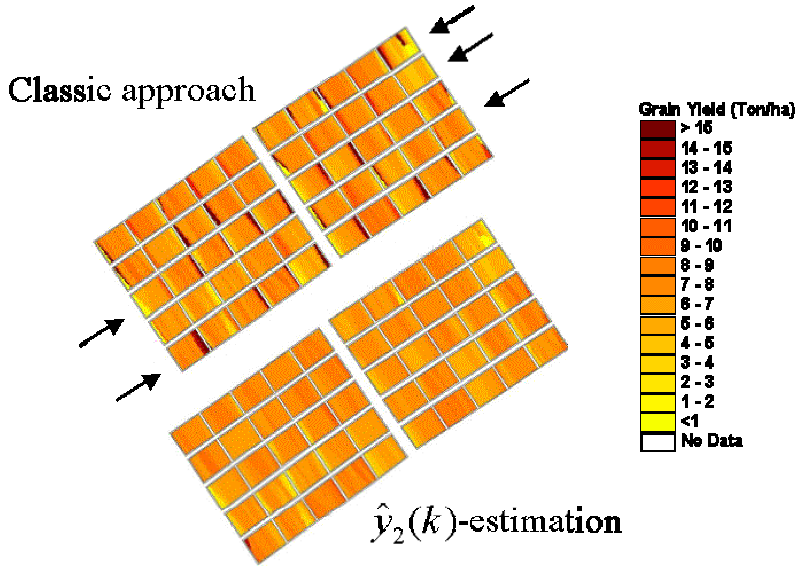

Figure 9. Comparison between grain yield maps constructed with classical approach, consisting of a optimal timeshift between mass flow and surface flow together with the model based $\hat{y}_2(k)$-estimation (Maertens et al., 2000)

7. CONCLUSIONS

A method is proposed to model combine grain flow by means of physical insight and experimental data. This experimental information can be provided by the constructor, since this kind of tests must be carried out to evaluate new designs of machine elements. When the machine elements are connected in an analytical way, a global dynamic flow model of the harvester is achieved, providing information about the response of the global model on feedrate variations. After implementing this model in simulation software, a linear approximation can be extracted. This linear transfer function in combination with a simplified return loop system can be used for purposes of signal processing.

Two model based grain yield estimations have been presented.

- The first one, based on the inverse dynamics of the system, delivers a dynamic correction for each type of feedrate variation. The presence of high frequency noise, makes this method less robust towards measurement noise. By this, an extra low pass filter must be installed.
- The second yield estimation, only delivers correction for variations of the surface flow. This method is inherently more robust and no extra filters are needed.

In fact, a combination of both estimation techniques can be seen as complementary with respect to grain yield variations from different origins. By introducing the appropriate rules for selecting the estimator, an optimal online solution can be installed for all kind of harvesting conditions.

ACKNOWLEDGEMENTS

The authors gratefully acknowledge the I.W.T. (Instituut voor Wetenschappelijk Technologisch onderzoek) for the financial support through doctoral grant No. 001249. This study has been made possible through cooperation with New Holland Belgium.

REFERENCES

Blackmore, S. and Moore, M. 1999. Remedial correction of yield map data. *Precision Agriculture* 1:53-66.

Birrell, S.; Sudduth, K.A. and Borgelt, S.C. 1996. Comparison of sensors and techniques for crop yield mapping. *Computers and Electronics in Agriculture* 14: 215-233.

Gregory, J.M. and Fedler, C.B. 1987. Mathematical relationship predicting grain separation in combines. *Transactions of the ASAE* 30(6):1600-1604.

Huynh, V.M. and Powell, T.E. 1978. Cleaning shoe performance prediction. ASAE Paper No. 78-1565. St. Joseph, Mich.: ASAE.

Maertens, K; Reyniers, M; De Baerdemaeker, J.; Ramon H. and De Keyser R. 2000. Grain yield mapping on a combine harvester: a model based approach. In*Proc. 2nd IFAC/CIGR International Workshop on Bio-Robotics*, 299-304. Osaka, 25-26 November.

Maertens, K; De Baerdemaeker, J.; Ramon, H and De Keyser R. 2001a. An analytical grain flow model for a combine harvester, Part I: Design of the Model. *Journal of Agricultural Engineering Research* 79(1)-63.

Maertens, K; De Baerdemaeker, J.; Ramon, H and De Keyser R. 2001b. An analytical grain flow model for a combine harvester, Part II: Analysis and Application of the Model. *Journal of Agricultural Engineering Research* (In Press).

Maertens, K; De Baerdemaeker, J. 2001. Flow rate based prediction of threshing process in combine harvesters. *Transactions of the ASAE* (Submitted).

Searcy, S.; Schueller, J.K.; Bae, Y.H.; Borgelt, S.C. and Stout, B.A. 1989. Mapping of spatially variable yield during grain combining. *Transactions of the ASAE* 32(3): 826-829.

Schoukens, J.; Dobrowiecki, T. and Pintelon, R. 1998. Parametric and non-parametric identification of linear systems in the presence of non-linear distortions. A frequency domain approach. *IEEE Transactions on Automatic Control* AC-43(2):176-190.

Trollope, J.R. 1982. A mathematical model of the threshing process in a conventional combine thresher. *Journal of Agricultural Engineering Research* 27:119-130.

Van Meirvenne, M; Hofman, G and Demyttenaere, P. 1990. Spatial variability of nitrogen fertilizer application and wheat yield. *Fertilizer Research* 23:15-23.

Vansichen, R. and De Baerdemaeker, J. 1992. Signal processing and system dynamics for continuous yield measurements on a combine. In*Proc. of Int. Conf. on Agricultural Engineering*, Uppsala, Paper No 92-0601.